High-resolution and high-sensitivity phase-contrast imaging by focused hard x-ray ptychography with a spatial filter

Yukio Takahashi, Akihiro Suzuki, Shin Furutaku, Kazuto Yamauchi, Yoshiki Kohmura, and Tetsuya Ishikawa

Citation: Applied Physics Letters **102**, 094102 (2013); doi: 10.1063/1.4794063
View online: http://dx.doi.org/10.1063/1.4794063
View Table of Contents: http://scitation.aip.org/content/aip/journal/apl/102/9?ver=pdfcov
Published by the AIP Publishing

High-resolution and high-sensitivity phase-contrast imaging by focused hard x-ray ptychography with a spatial filter

Yukio Takahashi,[1,a)] Akihiro Suzuki,[1] Shin Furutaku,[1] Kazuto Yamauchi,[1] Yoshiki Kohmura,[2] and Tetsuya Ishikawa[2]
[1]*Department of Precision Science and Technology, Graduate School of Engineering, Osaka University, 2-1 Yamada-oka, Suita, Osaka 565-0871, Japan*
[2]*RIKEN SPring-8 Center, 1-1-1 Kouto, Sayo-cho, Sayo, Hyogo 679-5148, Japan*

(Received 10 December 2012; accepted 19 February 2013; published online 4 March 2013)

We demonstrate high-resolution and high-sensitivity x-ray phase-contrast imaging of a weakly scattering extended object by scanning coherent diffractive imaging, i.e., ptychography, using a focused x-ray beam with a spatial filter. We develop the x-ray illumination optics installed with the spatial filter to collect coherent diffraction patterns with a high signal-to-noise ratio. We quantitatively visualize the object with a slight phase shift ($\sim\lambda/320$) at spatial resolution better than 17 nm in a field of view larger than $\sim 2 \times 2\,\mu\text{m}^2$. The present coherent method has a marked potential for high-resolution and wide-field-of-view observation of weakly scattering objects such as biological soft tissues. © *2013 American Institute of Physics*. [http://dx.doi.org/10.1063/1.4794063]

Imaging with hard x rays is an indispensable tool for the nondestructive and quantitative visualization of the internal structures of thick specimens in medicine, materials science, and biology. In conventional hard x-ray imaging, image contrast results from the variations in x-ray absorption arising from density differences and the variations in composition and thickness of the object; however, the sensitivity is low, particularly for materials consisting of light elements, such as soft biological tissue, polymers, and carbon-fiber composites because of a little absorption. Phase contrast in x-ray imaging was first reported in 1995,[1] which has a high sensitivity beyond the absorption contrast. The x-ray phase-contrast imaging now attracts interest in potential medical applications.[2,3] However, the spatial resolution of hard x-ray imaging techniques for weak objects is still poor and is currently limited by x-ray focusing optics.

Coherent x-ray diffractive imaging[4] (CXDI) is an x-ray phase-contrast imaging without a lens beyond the spatial resolution of conventional x-ray microscopes and is based on coherent x-ray diffraction and phase retrieval calculation. CXDI in the original concept has a plane-wave geometry, in which the sample is illuminated with an x-ray plane wave. Up to now, plane-wave CXDI has been applied to the observation of weakly scattering objects of biological specimens.[5] Plane-wave CXDI has a significant limitation, that is, the sample must be an isolated object less than a few micrometers in size. Scanning CXDI, which is called x-ray ptychography, became a breakthrough that solved this limit.[6] A probe is scanned across the sample and the diffraction pattern is observed at each beam position. Recently, high-resolution ptychography using focused x-ray beams[7,8] and biological applications in two[9] and three dimensions[10] have been reported.

A daunting task for x-ray ptychography at present is high-resolution observation of weakly scattering objects such as soft biological tissue. In x-ray ptychography, the reconstruction of data from weakly scattering specimens is known to be difficult compared with that in the plane-wave CXDI, because of the diffraction of the probe, i.e., the signal from the specimen is not only similarly weak, but the data are also dominated by the diffraction of the probe, which often produces artifacts. To suppress the appearance of the artifact, some schemes were proposed,[11] in which a round scan is used for ptychographic data collection instead of a raster scan or the reference sample is measured to obtain an initial probe for the reconstruction of the weakly scattering specimens. However, the main problem, i.e., the low signal-to-noise (S/N) ratio of diffraction patterns of the specimen, still exists.

In this letter, we report the demonstration of high-resolution x-ray ptychography of a weakly scattering extended object. We design and develop the illumination optics that combines the focusing mirrors with the spatial filter to collect ptychographic coherent diffraction patterns with extremely high S/N ratio. We visualize a slight phase shift ($\sim\lambda/320$) by x-ray ptychography installed with the illumination optics.

First, two-dimensionally focusing x-ray optics with a spatial filter was designed by the wave optical simulation. Kirkpatrick-Baez (KB) mirrors, which consist of two elliptical mirrors, were selected as the illumination optics because of their high focusing efficiency, which were designed so as to produce diffraction-limited focused x rays of ~100 nm spot size at an x-ray energy of ~8 keV. Figure 1(a) shows the schematic of the wave optical simulation for designing the spatial filter that is composed of cross slits. The wave propagation for only the vertical direction was calculated to decrease the computational complexity. A slit was positioned at the focal plane. Figure 1(b) shows the slit interval dependences of the intensity distribution observed at the detector plane. Fresnel diffraction due to the finite aperture of the mirror was derived in the calculation without the slit, while a part of the tail of the Fresnel diffraction is cut off in the calculation with the slit. As the slit interval becomes small, the cut-off q range becomes large and the intensities become

[a)]Electronic mail: takahashi@prec.eng.osaka-u.ac.jp; http://www-up.prec.eng.osaka-u.ac.jp/takahashi/.

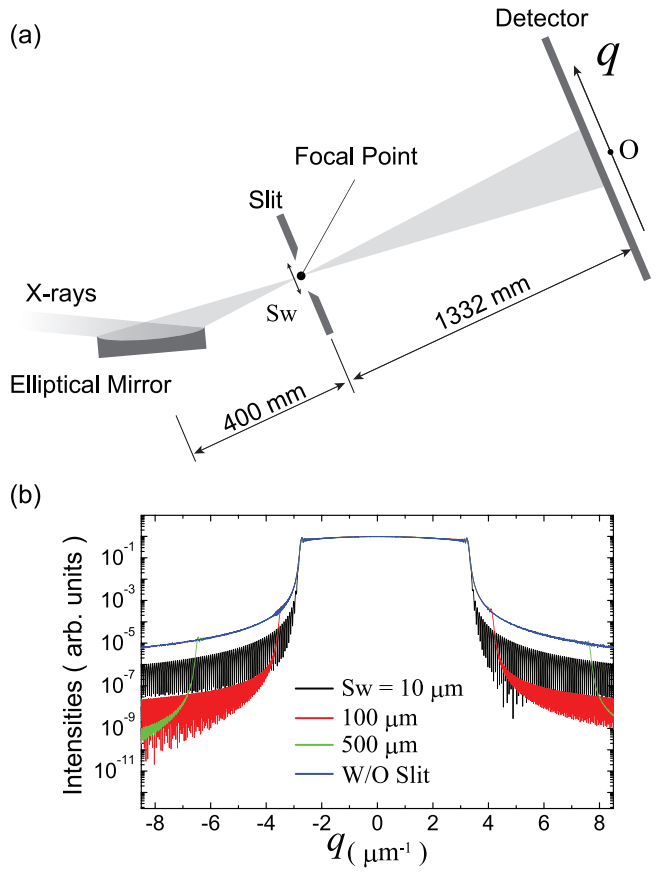

FIG. 1. (a) Schematic of the elliptical mirror for the vertical focusing, slit, and detector arrangement in the present simulation. (b) Slit interval (Sw) dependences of intensity distribution at the detector. $\boldsymbol{q}$ is defined as $|q| = 2\sin(\Theta/2)/\lambda$, where Θ is the scattering angle and λ is the x-ray wavelength.

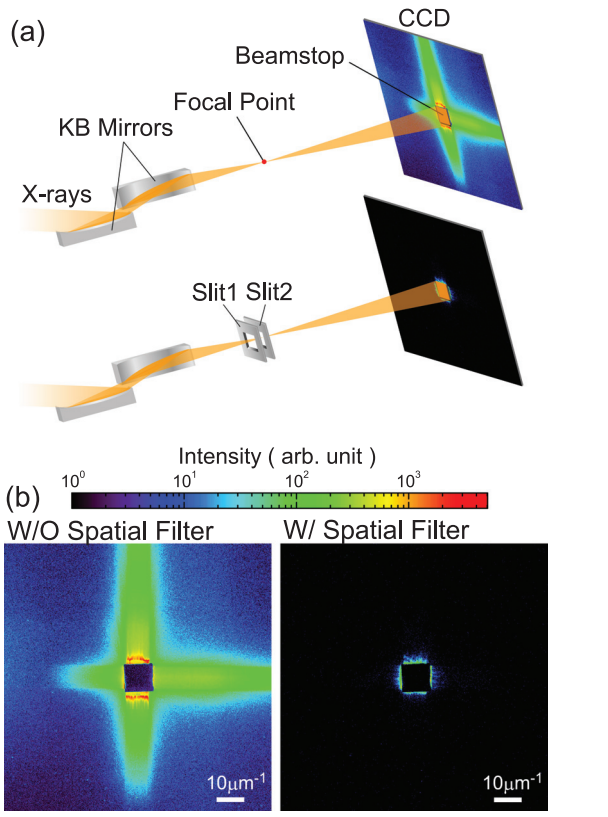

FIG. 2. (a) Schematic of the optical system for high-resolution x-ray ptychography without (upper) and with (lower) the spatial filter. The x rays of 8 keV were two-dimensionally focused using KB mirrors. Slit 1 ($70 \times 70\,\mu m^2$ hole) and slit 2 ($100 \times 100\,\mu m^2$ hole) were placed 1.5 and 0.5 mm upstream of the focal point, respectively. A CCD detector with a pixel size of $20 \times 20\,\mu m^2$ was placed 1332 mm downstream of the focal point. A direct beam stop was placed in front of the CCD detector. X-ray exposure time at each setup was 150 s. (b) Intensity distribution measured using a CCD detector in both setups.

higher at the high-q region owing to the increase in the photon of scattering x rays from the edge of the slit. Since the bright field at the small-q region is hidden by the beam stop in the experiment, it is understood that the optimum interval of the slit is $\sim$100 μm.

The performance of the illumination optics with a spatial filter was tested using synchrotron x rays at BL29XUL (Ref. 12) in SPring-8. Figure 2(a) shows the schematic of the experimental setup. 8 keV monochromatic x rays were focused to $\sim$100 nm (FWHM) spot size by KB mirrors. The flux of the focused x rays was $\sim 6 \times 10^7$ photons/s. The spatial filter was composed of two window slits, in which slit 1 and slit 2 are 20-μm-thick tantalum (Ta) foil with a $70 \times 70\,\mu m^2$ hole and 10-μm-thick Ta foil with a $100 \times 100\,\mu m^2$ hole, respectively, which were produced using the focused ion beam. Slit 1 and slit 2 were positioned close to the focal point, where the roles of slit 1 and slit 2 were to cut off the tail of the Fresnel diffraction from the mirrors and to cut off scattering x rays from slit 1, respectively. The intensity distribution at the far field was detected by the in-vacuum front-illuminated charge-coupled device (CCD) detector. Figure 2(b) shows the intensity distribution measured in both setups. The Fresnel diffraction from the mirrors was observed in the setup without the spatial filter. The x-ray intensities for right and upper directions are stronger than those for left and lower directions, which is attributable to the surface roughness on the mirrors. In the setup with the spatial filter, the x-ray intensities in the dark field decreased by two orders of magnitude compared with those in the setup without the spatial filter.

Next, the coherent diffraction patterns from a test object were measured using both setups. Figure 3(a) shows the SEM image of the test object. The test object is made of a 12-nm-thick Ta film with the smallest features of 17 nm lines and spaces, which simulates a weakly scattering extended specimen. The amount of phase shift of the $\sim$12-nm-thick Ta film at 8 keV is estimated to be $\sim$0.02 radian. The test object was located at the focal plane. Figure 3(b) shows the coherent diffraction patterns in the setup without and with the spatial filter. In the setup without the spatial filter, Fresnel diffraction from the mirrors is predominant. The diffraction from the test object was buried within the Fresnel diffraction. On the other hand, in the setup with the spatial filter, diffraction pattern from the test object with a high S/N ratio is observed. The present spatial filter system works well for measuring the coherent diffraction patterns with a high S/N ratio only from the weakly scattering object.

The ptychographic diffraction pattern data of the test object were collected in the setup with the spatial filter. The test object was illuminated in 9×9 overlapping fields of view, which were spaced by 150 nm. The data collection procedure is the same as that described in a previous report.[8]

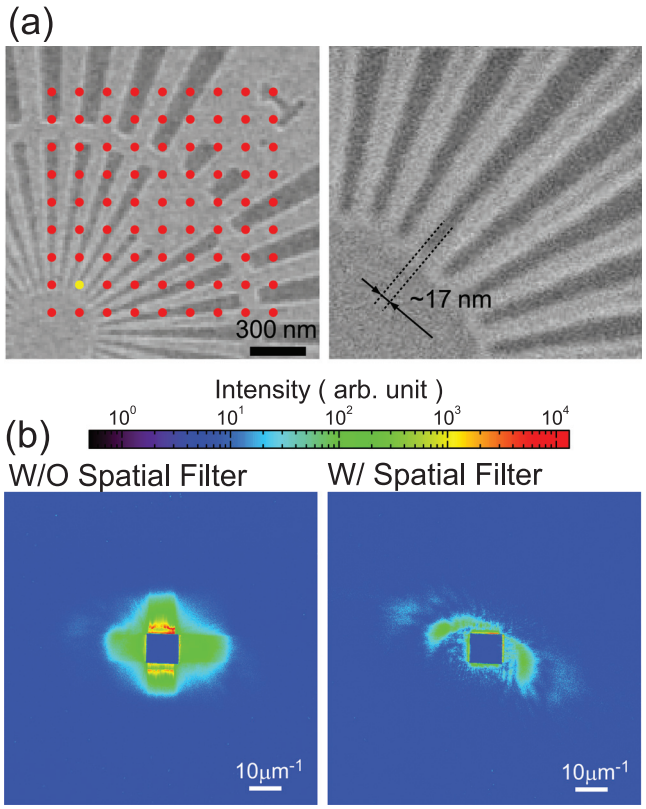

FIG. 3. (a) SEM image of the test object. Round dots indicate the x-ray irradiation positions. (Right) Enlarged SEM image of the area including the minimum structures. (b) Coherent diffraction patterns of the test object without the spatial filter and with the spatial filer. The x-ray illumination position is indicated by a light-colored dot in (a). X-ray exposure time at each setup was 150 s.

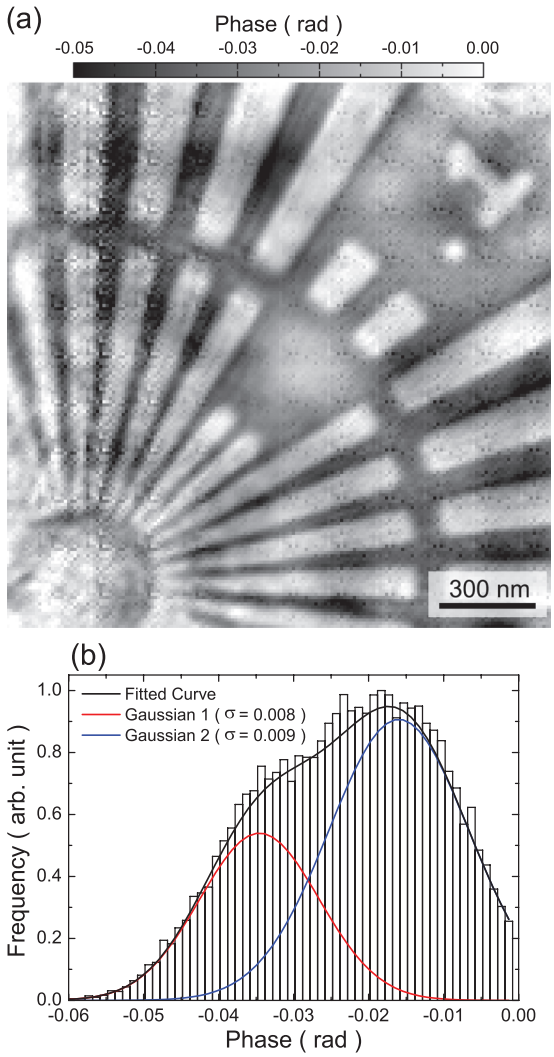

FIG. 4. (a) Reconstructed phase map of the test object by focused x-ray ptychography with the spatial filter. The pixel size is 10.0 nm. The total pixel number is 170 × 170. (b) Histogram of the phase distribution of (a), which was fitted by a composite function of two Gaussian functions.

X-ray exposure times at each position were 400 s. The total measurement time was ~16.5 h. The complex transmission function of the test object was reconstructed from the 81 diffraction patterns using the extended ptychographical iterative engine[13] within the weak phase object approximation.[11] The reconstruction was started from a flat object of unit transmission and an illumination wave field that was derived by x-ray ptychography of the known nanostructured sample. The iterative process was continued for up to 1×10^4 iterations.

Figure 4(a) shows the reconstructed phase map of the complex transmission function of the test object of 10.0 nm pixel size. The weak phase object approximation is justified since the amount of phase shift is less than 0.02 radian. 17 nm line-and-space structures are visible in the field of view larger than $2 \times 2\,\mu m^2$, which indicates that the spatial resolution of the present image is better than 17 nm. The reconstructed phase map exhibits high noise and non-uniformity in some regions compared to the SEM image in Fig. 3(a) and includes periodic artifacts. The noise and the non-uniformity are mainly due to the photon shot noise of scattering x rays. The periodic artifacts result from the translation symmetry of the raster scan. Figure 4(b) shows the histogram of the phase distribution of Fig. 4(a). The histogram was fitted by a composite function of two Gaussian functions. It has been reported that phase resolution is defined by measuring the standard deviation (σ) of the Gaussian fit.[14] According to this definition, the phase resolution of the present image is better than 0.01 radian, which is the best sensitivity achieved by hard x-ray phase-contrast imaging as for as we know. In addition, the interval at the peak top position is 0.018 radian, approximately corresponding to the calculated value. This means that the present coherent imaging technique is also quantitative method.

In conclusion, we have established a high-resolution and high-sensitivity phase-contrast imaging technique by focused x-ray ptychography using a spatial filter. We quantitatively visualized the extended object at spatial resolution better than 17 nm and phase resolution better than 0.01 radian in a field of view larger than $2 \times 2\,\mu m^2$. The phase shift of $\sim\lambda/320$ corresponds to that of a ~100-nm-thick amorphous carbon at an x-ray energy of 8 keV, which indicates that the present phase-contrast imaging techniques can be used to observe weakly scattering objects such as biological soft tissues and polymer materials at ~10 nm resolution. At present, the image quality, the spatial resolution, the field of view, and the measurement time are mainly limited by the flux of coherent x rays. We believe that this limitation can be overcome using a highly brilliant x-ray source such as an ultimate storage ring or an energy recovery linac in the near future.

This work was supported by a Grants-in-Aid for Scientific Research (Grants No. 24651137 and No. 23102504), Core Research for Evolutional Science and Technology, the Global COE Program "Center of Excellence for Atomically Controlled Fabrication Technology," and X-ray Free Electron Laser Priority Strategy Program from the Ministry of Education, Culture, Sports, Science and Technology.

[1]A. Snigirev, I. Snigireva, V. Kohn, S. Kuznetsov, and I. Schelokov, Rev. Sci. Instrum. **66**, 5486 (1995).
[2]S. W. Wilkins, T. E. Gureyev, D. Gao, A. Pogany, and A. W. Stevenson, Nature (London) **384**, 335 (1996).
[3]A. Momose, T. Takeda, Y. Itai, and K. Hirano, Nat. Med. **2**, 473 (1996).
[4]J. Miao, P. Charalambous, J. Kirz, and D. Sayre, Nature (London) **400**, 342 (1999); H. N. Chapman and K. A. Nugent, Nat. Photonics **4**, 833 (2010).
[5]J. Miao, K. O. Hodgson, T. Ishikawa, C. A. Larabell, M. A. LeGros, and Y. Nishino, Proc. Natl. Acad. Sci. U.S.A. **100**, 110 (2003); Y. Nishino, Y. Takahashi, N. Imamoto, T. Ishikawa, and K. Maeshima, Phys. Rev. Lett **102**, 018101 (2009); J. Nelson, X. Huang, J. Steinbrener, D. Shapiro, J. Kirz, S. Marchesini, A. M. Neiman, J. J. Turner, and C. Jacobsen, Proc. Natl. Acad. Sci. U.S.A. **107**, 7235 (2010); H. Jiang, C. Song, C. C. Chen, R. Xu, K. S. Raines, B. P. Fahimian, C. H. Lu, T. K. Lee, A. Nakashima, J. Urano, T. Ishikawa, F. Tamanoi, and J. Miao, Proc. Natl. Acad. Sci. U.S.A. **107**, 11234 (2010).
[6]J. M. Rodenburg, A. C. Hurst, A. G. Cullis, B. R. Dobson, F. Pfeiffer, O. Bunk, C. David, K. Jefimovs, and I. Johnson, Phys. Rev. Lett. **98**, 034801 (2007).
[7]P. Thibault, M. Dierolf, A. Menzel, O. Bunk, C. David, and F. Pfeiffer, Science **321**, 379 (2008); A. Schropp, P. Boye, J. M. Feldkamp, R. Hoppe, J. Patommel, D. Samberg, S. Stephan, K. Giewekemeyer, R. N. Wilke, T. Salditt, J. Gulden, A. P. Mancuso, I. A. Vartanyants, E. Weckert, S. Schöder, M. Burghammer, and C. G. Schroer, Appl. Phys. Lett. **96**, 091102 (2010); A. Schropp, R. Hoppe, J. Patommel, D. Samberg, F. Seiboth, S. Stephan, G. Wellenreuther, G. Falkenberg, and C. G. Schroer, Appl. Phys. Lett. **100**, 253112 (2012).
[8]Y. Takahashi, A. Suzuki, N. Zettsu, Y. Kohmura, Y. Senba, H. Ohashi, K. Yamauchi, and T. Ishikawa, Phys. Rev. B **83**, 214109 (2011).
[9]K. Giewekemeyer, P. Thibault, S. Kalbfleisch, A. Beerlink, C. M. Kewish, M. Dierolf, F. Pfeiffer, and T. Salditt, Proc. Natl. Acad. Sci. U.S.A. **107**, 529 (2010).
[10]M. Dierolf, A. Menzel, P. Thibault, P. Schneider, C. M Kewish, R. Wepf, O. Bunk, and F. Pfeiffer, Nature **467**, 436 (2010).
[11]M. Dierolf, P. Thibault, A. Menzel, C. M. Kewish, K. Jefimovs, I. Schlichting, K. König, O. Bunk, and F. Pfeiffer, New J. Phys. **12**, 035017 (2010).
[12]K. Tamasaku, Y. Tanaka, M. Yabashi, H. Yamazaki, N. Kawamura, M. Suzuki, and T. Ishikawa, Nucl. Instrum. Methods Phys. Res. A **467-468**, 686 (2001).
[13]A. M. Maiden and J. M. Rodenburg, Ultramicroscopy **109**, 1256 (2009).
[14]C. T. Putkunz, J. N. Clark, D. J. Vine, G. J. Williams, M. A. Pfeifer, E. Balaur, I. McNulty, K. A. Nugent, and A. G. Peele, Phys. Rev. Lett. **106**, 013903 (2011).